

## Efficient numerical method for various geometries of gas lubricated bearings

R.H.M. van der Stegen and H. Moes<sup>a</sup>

<sup>a</sup>Tribology Group, Dept. of Mechanical Engineering, University of Twente, P.O. Box 217, 7500 AE Enschede, The Netherlands

This paper discusses the development of a numerical solver for the Reynolds equation in aerodynamic lubricated bearings, utilizing a finite difference method with multigrid. The advantages of the numerical method are that the number of operations and the memory capacity needed are almost proportional to the number of gridpoints involved. It is second order accurate and can cope with various bearing geometries. A survey is also given of the implemented modifications of the Reynolds equation. The efficiency of the method is demonstrated by two examples, namely: the dynamic tracking of the centre of a herringbone grooved journal bearing and the equilibrium position of a hard disk slider.

### 1. Introduction

An analytical solution of the Reynolds equation for gas lubricated bearings is only available in some special situations. Therefore, in general, a numerical approach is required.

During the last decades several methods have been proposed for discretising the Reynolds equation. They may be divided in two groups, namely "finite element methods (FEMs)" and "finite difference methods (FDMs)". An early survey of numerical methods was published by Castelli and Pirvics (1968). Recently, substantially improved methods have been introduced. Useful FEMs have been developed, among others, by Bonneau, Huitric and Tournerie (1993) and by Nguyen (1991). The advantage of the FEMs is that they can be applied to a large variety of geometries. Nevertheless, the FDM is still used; see for example Lipschitz, Basu and Johnson (1991).

The numerical solution of the set of equations, constructed with the methods mentioned above, is quite expensive for a large number of points, i.e. the number of operations and the memory capacity needed are at least  $O(n^2)$ , with  $n$  the number of grid points involved. The numerical simulation is further complicated by the nonlinear character of the Reynolds equation and the wide velocity range of gas bearings. However, a multi-grid solver in combination with a FDM decreases

the number of operations and the memory capacity needed and makes them directly proportional to the number of grid points involved. Therefore, this method is applied for solving the Reynolds equation.

A numerical method is presented that solves the Reynolds equation second order accurate, in arbitrarily shaped bearings. The grid points are equally spaced on the domain, but the location of these points is independent of the shape of the bearing surfaces.

To begin with, the bearing model will be presented and some possible modifications of the Reynolds equation are specified that extend its applicability. Next the numerical solver will be composed of a FDM and a multigrid solver. Finally two applications will be shown, namely a hard disk slider and a herringbone journal bearing.

### 2. Bearing model

Let us consider a model of a gas lubricated bearing of which the behaviour is to be analysed.

If the bearing is not defined in a rectangular domain, it has to be transformed onto it by a co-ordinate transformation. For instance, a journal bearing is unwrapped to a plain bearing and a thrust bearing is described in polar coordinates.

Figure 1 shows a schematic representation of a

bearing on the domain  $((0, l_x), (0, l_y))$ . The surfaces may have waviness, pockets or alternative groove geometries, like straight, herringbone or spiral grooves. The surfaces move in the tangential direction with a constant velocity  $\underline{u}$ .

The bearing clearance ( $h$ ) is a function of the given surface geometry and a global function with some degrees of freedom. Three combinations are of special interest, namely:

- the static solution; with no degrees of freedom for the clearance,
- the equilibrium solution; a steady state global function needs to be solved for every degree of freedom of the clearance,
- the time dependent solution; a transient global function needs to be solved for every degree of freedom of the clearance.

The boundary conditions complete the model. The values of the pressure ( $p$ ) are known along the external boundary parallel to the  $x$ -axis (Dirichlet boundary). The boundary parallel to the  $y$ -axis can, respectively, be of the Neumann or the Dirichlet type:

- a cyclic bearing condition, i.e.  $p(x=0, y) = p(x=l_x, y)$ ,
- a slider bearing condition, i.e. the pressures  $p(x=0, y)$  and  $p(x=l_x, y)$  are known.

Algorithms have been derived for the six possible combinations.

### 3. Lubrication model

The Reynolds equation is generally used to describe the behaviour of the lubricant film. It is derived from the Navier Stokes equations and the continuity equation by assuming very thin gaps. However, modifications can be made in order to extend the applicability of the Reynolds equation.

The Reynolds equation is written in the divergence form, neglecting the external forces, and reads:

$$\nabla \cdot \left( \frac{\rho h^3}{12\eta} \nabla p - \frac{\rho h \underline{u}}{2} \right) - \frac{\partial \rho h}{\partial t} = 0, \quad (1)$$

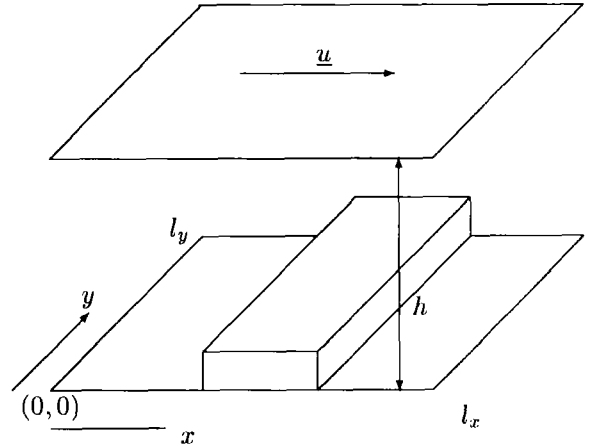


Figure 1. Schematic presentation of a bearing.

with  $\underline{u}$  and  $h$  for the sum velocity of the bearing surfaces and the clearance, respectively. The time is  $t$ . The pressure, the density and the viscosity are denoted by respectively,  $p$ ,  $\rho$  and  $\eta$ .

Further it is assumed that the flow is isoviscous and isothermal. Therefore the density  $\rho$  may be replaced by the pressure  $p$  according to  $p = \rho R_g \vartheta$ , with  $\vartheta$  and  $R_g$  for the temperature and the gas constant.

Because a number of assumptions have been made during the derivation, restrictions are necessary in order to obtain an accurate approximation for the flow in a clearance.

Special attention is paid to the flow of gas in an ultra thin gap, like between a hard disk and a slider. The original Reynolds equation is restricted to flows where the molecular mean free path is negligible as compared to the thickness of the gap. Whenever both lengths are comparable, slip between the gas and the wall produces an effect that is similar to a reduction of the viscosity.

The Reynolds equation can be adopted to ultra thin gaps by applying well known theories. The characteristic parameter is the Knudsen number ( $Kn$ ). It represents the ratio between the mean free path ( $\lambda$ ) and the gap ( $h$ ):

$$Kn = \frac{\lambda}{h}. \quad (2)$$

A first order approximation of the molecular slip velocity may be derived from the kinetic gas theory. It was implemented in the Reynolds equation by Burgdorfer (1959):

$$\nabla \cdot \left( \left( \frac{\rho h^3}{12\eta} + \frac{\lambda_0 p_0 h^2}{2\eta} \right) \nabla p - \frac{\rho h \underline{u}}{2} \right) - \frac{\partial \rho h}{\partial t} = 0, (3)$$

with  $\lambda_0$  for the mean free molecular path at the pressure  $p_0$ .

Higher order approximations for the slip in the Reynolds equation were investigated by Hsia and Domoto (1983) and Mitsuya (1993). Fukui and Kaneko (1988) derived a molecular gas equation which looks familiar to the Reynolds equation. This equation is specifically suited for very large Knudsen numbers.

Other well known adaptations are the incorporation of centrifugal effects (Pinkus and Lund, 1981) and turbulence (Taylor and Dowson, 1974). These models were originally derived for incompressible flow, but may quite as well be used for compressible flow.

All these modifications of the Reynolds equation will be neglected in the construction of the numerical method.

#### 4. Numerical procedure

A numerical procedure will now be presented that solves the Reynolds equation with second order accuracy. It is a combination of a FDM-discretisation and a multigrid method.

Point of departure is the dimensionless Reynolds equation in cartesian coordinates, a non-linear differential operator. Since velocity in one direction is assumed, this equation reads:

$$\frac{\partial}{\partial X} \frac{d}{2} \frac{\partial P^2}{\partial X} + \gamma \frac{\partial}{\partial Y} \frac{d}{2} \frac{\partial P^2}{\partial Y} - \Lambda \frac{\partial a P}{\partial X} - \sigma \frac{\partial a P}{\partial T} = 0. (4)$$

The variable  $P$  represents the dimensionless pressure and needs to be solved. The diffusion coefficient  $d$  and the advection coefficient  $a$  are known functions of the dimensionless bearing clearance  $H$  and the position in the bearing.  $\gamma$  is the squared aspect ratio.  $\Lambda$  and  $\sigma$  are the dimensionless velocity and the dimensionless squeeze number.

#### 4.1. Discretisation

The discretisation of the Reynolds equation is based on the filmthickness *between* two grid points ( $d_{i\pm\frac{1}{2}}$  and  $a_{i\pm\frac{1}{2}}$ ), instead of coefficients *in* the grid points. These two discretisations lead to different solutions when an internal boundary is crossed. The first discretisation needs only one relaxation point to cross a boundary, while the second one invariably needs a number of points. Therefore the position of the discontinuity is presented more accurately with the first method, resulting in a more accurate solution.

A first and a second order accurate discretised Reynolds equation (in stencil notation:  $L(P)_{i,j,k} = f_{i,j,k}$ ) are presented in appendix A.

#### 4.2. Multigrid

Multigrid has originally been introduced for an isotropic function  $P$ , with a smooth behaviour of  $\nabla P$ . The Reynolds equation for gas lubrication can be non-isotropic and shows strongly discontinuous coefficients across internal boundaries. This requires special measures for the solver.

A number of so-called black box multigrid methods have been proposed that overcome the difficulties just mentioned. Two basic methods of adaptation of the solver are available that regain the desired convergence rate.

Zeeuw (1990) has developed a multigrid solver based on matrix operations to obtain the coarse grid operator. Therefore this method can only be applied if the Reynolds equation has been linearised. It results in a nine-point relaxation stencil on coarse grids. The preliminary work needed for this method is quite extensive because matrices must be inverted.

An alternative method was proposed by Alcouffe, Brandt, Dendy and Painter (1981). A multigrid solver was derived for a Laplace equation with strongly discontinuous coefficients. The method did not include advection and a nonlinear equation. The advantage of the method is that it uses a five point relaxation stencil on coarse grids and does not need matrix inversions.

The algorithm presented is based on the work of Alcouffe et al. (1981). It is implemented in the Full MultiGrid, Full Approximation Scheme (Brandt, 1984) for a nonlinear equation.

#### 4.2.1. Relaxation

The operator in a multigrid solver must be such that the relaxation is stable and an effective smoother. "Stable" means that every frequency component is reduced by the relaxation process. For multigrid efficiency in addition, good smoothing properties are essential, i.e. all high frequency components need to be reduced fast.

The preferred discretisation for the operator is the one with second order accuracy. However due to stability and smoothing requirements, its applicability is limited to regions where the diffusion derivative is larger than the advection derivative. On the contrary, the relaxation of the first order accurate scheme is stable and a good smoother. Therefore, when the second order scheme is not stable or not a good smoother and if a second order solution is needed, the first order is used and the accuracy is increased from first to second by introducing: "defect correction" (Khosla and Rubin, 1974).

Caution is needed along and across internal boundaries. These discontinuities cause locally large pressure gradients, depending on the geometry of the bearing and the bearing velocity. The safest method is to use first order discretisation with, if necessary, defect correction.

The type of relaxation depends on the ratio of the derivatives in the  $X$ - and  $Y$ -direction. If it is isotropic, a one point Gauss-Seidel relaxation can be used. In non-isotropic regions, Gauss-Seidel line-relaxation should be used.

#### 4.2.2. Intergrid transfer

The differences are described between the constructed intergrid transfer procedures and the implementation of Alcouffe et al. (1981). The guiding principle is the smooth behaviour of:  $\frac{d}{2}\nabla P^2 - \Lambda aP$ , which represents the mass flow.

The interpolation and restriction operators must prevent that information is averaged when crossing internal boundaries. A common choice for the restriction operator is applying the inverse of the interpolation operator for internal boundary problems. This choice is very expensive. Whereas a coarse approximation also gives satisfying results. The latter is based on a weighting with the reciprocal of the diffusion coefficients.

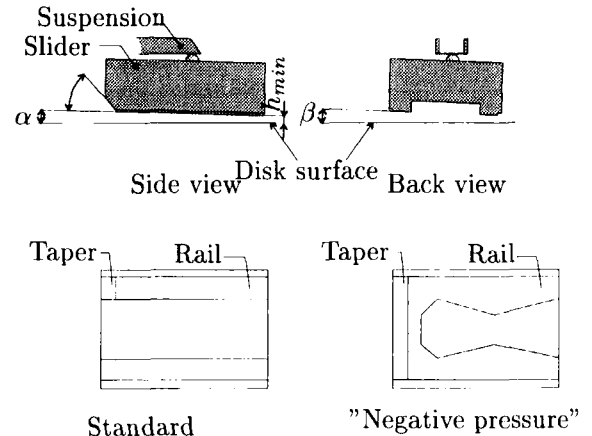


Figure 2. Slider geometry

The interpolation is based on the discretised operator.

The coarse grid operator is based on the discretisation of the fine grid operator. The method for calculating the advection and diffusion coefficients  $a$  and  $d$  was based on Alcouffe et al. (1981).

## 5. Applications

Two applications will be presented which are usually solved with different methods, namely a hard disk slider and a herringbone grooved journal bearing.

### 5.1. Hard disk sliders

The study of hard disk sliders has been stimulated by the minimisation of the hard disk dimensions. Several slider designs have been proposed, like the standard two rail slider (for example the IBM 3370) and the so-called "negative pressure slider". Sliders are often judged by their equilibrium position. Three degrees of freedom must be solved to find the equilibrium position, namely the minimal film thickness ( $h_{min}$ ), the pitch angle ( $\alpha$ ) and the roll angle ( $\beta$ ) (Figure 2).

The numerical method solves the pressure distribution with the equilibrium position of the slider. The degrees of freedom are solved most efficiently on the coarsest grid of a multigrid cycle

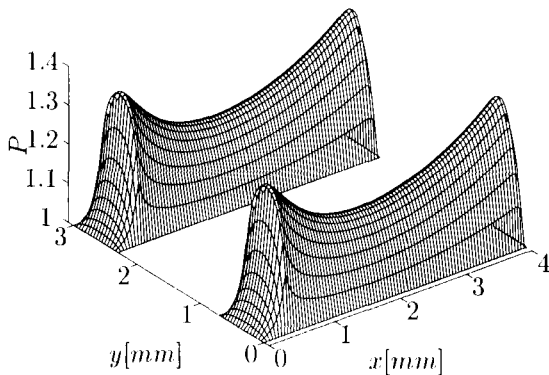


Figure 3. Pressure distribution under a IBM 3370 slider

(Venner, 1991). The equilibrium position is found in two steps. During the first step, the pressure distribution and the load balance are matched, when the finest level is level two. If the multigrid process contains three or more levels, the load and momentum are balanced.

The efficiency of the numerical procedure is demonstrated for an IBM 3370 slider, as well as for a negative pressure slider.

#### 5.1.1. IBM 3370 slider

The IBM 3370 slider is a standard two rail slider, with flat tapers. The area between the rails does not contribute to the lifting capacity.

Choi and Yoon (1994) developed a method for the prediction of the equilibrium position of a hard disk slider by using an optimization technique. Three standard sliders are discussed in their article, the results for the IBM 3370 will be compared with the present results. The notation and the equations of Choi are employed.

The method of Choi solves first the static pressure distribution. It needs 4 till 8 times more iterations to solve the pressure distribution with the equilibrium position.

The present method solves the standard slider on 7 succeeding levels. The coarsest grid has per rail  $1 \times 10$  nodes, the finest has  $127 \times 703$  nodes. The area between the rails is not disre-

level	$\alpha[\mu\text{rad}]$	$\beta[\mu\text{rad}]$	$h_{min}[\mu\text{m}]$
1	300.0	0.00	0.100
2	300.0	0.00	0.500
3	146.5	8.67	0.566
4	144.8	7.93	0.568
5	144.2	7.49	0.569
6	146.1	7.30	0.571
7	146.0	7.19	0.571
Ruiz	143.	7.1	0.55
Choi	145.	7.2	0.56

Table 1

Results for a IBM 3370 slider on 7 levels.

tised. The multigrid method needs two V-cycles with two pre and two post relaxations per level to solve the pressure distribution. Four cycles in total are needed to find the equilibrium position. This means that 16 relaxation of the finest grid are needed. However, on levels two and three, more cycles are needed, depending on the initial condition. The computational costs are very low for the low level cycles. Therefore these can be neglected when more than three levels are involved. The pressure distribution is given in Figure 3. Only one out of 64 gridpoints is shown.

The solution of the proposed method and the results of Choi and Yoon (1994) are listed in table 1. They compared their results with Ruiz and Bogy (1990). Excellent agreement of the minimal film thickness  $h_{min}$ , the pitch angle  $\alpha$  and the roll angle  $\beta$ , is seen between the three methods. On the finest level, level seven, the most accurate results are obtained. It is obvious that the differences between the solutions on succeeding levels become less when the level is finer. However the convergence of the solution is not exactly second order. This is caused by the switch from taper to rail, which in general does not coincide with a gridline. This reduces the convergence rate.

#### 5.1.2. Negative pressure slider

The so-called "negative pressure slider" consists of two rails with a threshold in between. Behind the threshold is a recessed area with a sub ambient pressure. This sucks the slider to the disk.

The negative pressure slider can be solved

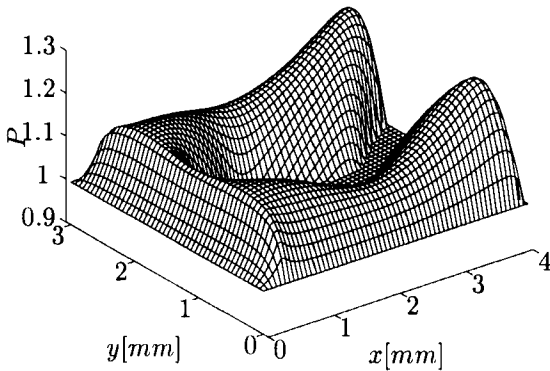


Figure 4. Pressure distribution under a negative pressure slider

level	$\alpha$ [ $\mu\text{rad}$ ]	$\beta$ [ $\mu\text{rad}$ ]	$h_{min}$ [ $\mu\text{m}$ ]
1	145.0	7.20	0.560
2	145.0	7.20	1.176
3	298.5	11.80	1.117
4	308.3	11.91	1.133
5	304.6	11.96	1.141
6	304.7	11.99	1.146

Table 2

Results for negative pressure slider on 6 levels.

with the same efficient method. The number of operations is a bit larger because multigrid W-cycles are needed instead of V-cycles. The complete slider is discretised, i.e. also the area between the rails. The coarsest level has 11 x 14 nodes, the finest 383 x 479 nodes. The pressure distribution is presented in Figure 4. Only one out of 64 points is plotted.

Geometries have not been published and therefore the results can not be compared. Table 2 presents the results on the six levels. The convergence of the solution is first order because the inaccurate description of the internal boundaries dominates the error in the solution.

level	$F_x$ [N]	$F_y$ [N]
1	-109.9	56.5
2	-147.3	56.7
3	-165.7	52.7
4	-174.9	49.0
5	-178.3	47.2
6	-180.6	46.0
7	-181.5	45.6

Table 3

Static results of a herringbone bearing.

## 5.2. Herringbone grooved journal bearing

Herringbone grooved journal bearings are applied in rotating machinery such as audio and video equipment. For gas bearings in particular, uncontrolled whirl can cause fatal damage to the bearing. Therefore the prediction of whirl is important for the designer. The stability of a bearing is simulated by solving the Reynolds equation and the equations of motion. The result is a transient prediction of the journal centre locus.

In a transient analysis, the previous solution is applied as an estimation for the next time step by the numerical method. The multigrid method is called "F-cycle". On the coarsest level 16 x 3 nodes are used, on the finest level (level 7) 1024 x 255 nodes. Three V-cycles, each with four relaxations at the finest level, are needed for the static solution. During the begin of the transient analysis, just two V-cycles within a F-cycle suffice; and when the high frequency oscillations have disappeared one V-cycle suffices.

The herringbone bearing under consideration has 8 grooves with a groove angle of 30 degrees and a land-groove ratio of 1. The groove depth is 1 [ $\mu\text{m}$ ] and the maximum eccentricity is 5 [ $\mu\text{m}$ ]. The grooved bearing is stationary and the smooth journal rotates with 100 [rps]. The attached rotor mass is 0.5 [kg]. The dimensions of the bearing are a diameter of 4 [cm] and a length of 3 [cm].

First, the static solution is solved for the dimensionless eccentricity  $(\epsilon_x, \epsilon_y) = (0.75, 0)$  of the herringbone bearing. The resulting forces  $F$  on the journal are given in table 3 for the seven levels. The convergence is reduced by the inaccurate description of the internal boundaries. This static

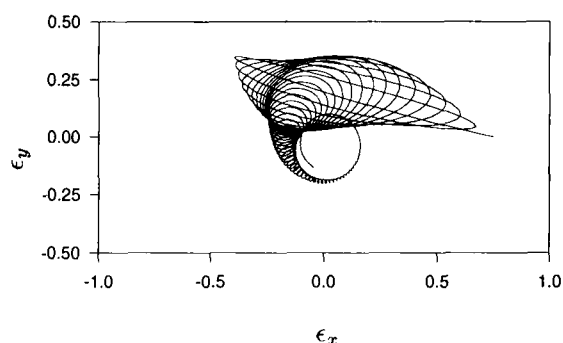


Figure 5. Journal centre path

solution is the departure point for the transient simulation of the loaded journal. Its centre path is given in figure 5.  $\Delta T$  is equal to  $\Delta X$ . In order to arrive at the limit cycle, thousands of time steps are needed, which is no problem for this efficient algorithm.

## 6. Conclusion

An efficient numerical method is derived for the static, equilibrium, and time dependent solution of a gas lubricated bearing. The method is based on a second order finite difference discretisation scheme and a multigrid solver. The efficiency of the method is demonstrated by the fact that the number of operations and the memory capacity needed are almost proportional to the number of gridpoints involved.

The method has been shown to be well suited for taking into account compressibility and complex geometries. The gridpoints are equally spaced on the domain. A geometry that is not smooth is therefore represented with first order accuracy because the exact location of the discontinuity can not be represented by the discretisations.

The method is applied to two examples, namely a hard disk slider and a herringbone grooved journal bearing. The equilibrium position of the slider is obtained with the same efficiency, independent of the geometry. The equilibrium of a slider requires the double amount of work of the static

solution. In a transient simulation of a herringbone bearing, the previous pressure distribution is applied as an estimation for the next distribution. In combination with a multigrid "F-cycle", this reduces substantially the number of operations per timestep as compared to a static solution.

## Acknowledgement

The authors would like to thank their colleagues of the Tribology Group and A. Reusken of the Eindhoven University of Technology in the Netherlands for their contributions, discussions and suggestions.

## Nomenclature

$a$	advection coefficient
$d$	diffusion coefficient
$f$	right hand side term
$F$	force
FDM	finite difference method
FEM	finite element method
$h(H)$	clearance ( $h = h_0 H$ )
$Kn$	Knudsen number
$l$	length
$L$	relaxation operator
$n$	number of gridpoints
$p(P)$	pressure ( $p = p_0 P$ )
$R_g$	gas constant
$t(T)$	time ( $t = \frac{T l_x}{u}$ )
$\underline{u}$	sumvelocity
$x, y(X, Y)$	cartesian coordinates ( $x = l_x X, y = l_y Y$ )
$\Delta X, \Delta T$	stepsizes
$\alpha$	pitch angle
$\beta$	roll angle
$\epsilon$	eccentricity
$\gamma$	squared aspect ratio ( $= \frac{l_x^2}{l_y^2}$ )
$\eta$	viscosity
$\lambda$	molecular mean free path
$\Lambda$	bearing velocity number ( $= \frac{6\eta u l_x}{p_0 h_0^2}$ )
$\rho$	density
$\vartheta$	temperature
$\sigma$	squeeze number ( $= \frac{12\eta u l_x}{p_0 h_0^2}$ )

**Sub- and superscripts**

<i>min</i>	minimum value
<i>x</i>	index in <i>x</i> direction
<i>y</i>	index in <i>y</i> direction
<i>i</i>	index in <i>X</i> direction
<i>j</i>	index in <i>Y</i> direction
<i>k</i>	index in <i>T</i> direction
0	reference value
1	first order accurate
2	second order accurate

**A. Discretisation**

The discretisation of the operators  ${}^2L(P)_{i,j,k}$  and  ${}^1L(P)_{i,j,k}$  is given only in *X*- and *T*-direction, with  $X = i\Delta X$ , and  $T = k\Delta T$ . The second order accurate operator is:  ${}^2L^h(P)_{i,k} =$

$$\begin{aligned} & \left. \frac{d_{i+\frac{1}{2}}(P_{i+1}^2 - P_i^2) - d_{i-\frac{1}{2}}(P_i^2 - P_{i-1}^2)}{2(\Delta X)^2} \right|_k \\ & - \Lambda \left. \frac{a_{i+\frac{1}{2}}(P_{i+1} + P_i) - a_{i-\frac{1}{2}}(P_i + P_{i-1})}{2\Delta X} \right|_k \\ & - \sigma \left. \frac{3a_k P_k - 4a_{k-1} P_{k-1} + a_{k-2} P_{k-2}}{2\Delta T} \right|_i. \end{aligned} \quad (5)$$

Alternatively the operator  ${}^1L^h(P)_{i,k}$  is used:

$$\begin{aligned} & \left. \frac{d_{i+\frac{1}{2}}(P_{i+1}^2 - P_i^2) - d_{i-\frac{1}{2}}(P_i^2 - P_{i-1}^2)}{2(\Delta X)^2} \right|_k \\ & - \Lambda \left. \frac{a_{i+\frac{1}{2}} P_i - a_{i-\frac{1}{2}} P_{i-1}}{\Delta X} \right|_k \\ & - \sigma \left. \frac{3a_k P_k - 4a_{k-1} P_{k-1} + a_{k-2} P_{k-2}}{2\Delta T} \right|_i. \end{aligned} \quad (6)$$

The advection and diffusion coefficients *a* and *d* are functions of the dimensionless bearing clearance:

$$d_{i+\frac{1}{2},j} = \frac{1}{2}(H_{i+\frac{1}{2},j-\frac{1}{2}}^3 + H_{i+\frac{1}{2},j+\frac{1}{2}}^3), \quad (7)$$

$$a_{i+\frac{1}{2},j} = H_{i+\frac{1}{2},j}. \quad (8)$$

**REFERENCES**

Alcouffe, R. E., Brandt, A., Dendy, J. E. and Painter, J. W. (1981). The multi-grid method for the diffusion equation with strongly discontinuous coefficients, *SIAM J. Sci. Stat. Comput.* **2**(4): 430-454.

Bonneau, D., Huitric, J. and Tournerie, B. (1993). Finite Element Analysis of Grooved Gas Thrust Bearings and Grooved Gas Face Seals, *Journal of Tribology* **115**: 348-354.

Brandt, A. (1984). *Multigrid Techniques: 1984 Guide with Applications to Fluid Dynamics*, Gesellschaft fuer Mathematik und Datenverarbeitung MBH, Bonn.

Burgdorfer, A. (1959). The Influence of the Molecular Mean Free Path on the Performance of Hydrodynamic Gas Lubricated Bearings, *Journal of Basic Engineering* **81**: 94-100.

Castelli, V. and Pirvics, J. (1968). Review of Numerical Methods in Gas Bearing Film Analysis, *Journal of Lubrication Technology* **90**: 777-792.

Choi, D.-H. and Yoon, S.-J. (1994). Static Analysis of Flying Characteristics of the Head Slider by Using an Optimazation Technique, *Journal of Tribology* **116**: 90-94.

Fukui, S. and Kaneko, R. (1988). Analysis of Ultra-Thin Gas Film Lubrication Based on Linearized Boltzmann Equation: First Report - Derivation of a Generalized Lubrication Equation Including Thermal Creep Flow, *Journal of Tribology* **110**: 253-261.

Hsia, Y. T. and Domoto, G. A. (1983). An Experimental Investigation of Molecular Rarefaction Effects in Gas Lubricated Bearings at Ultra-Low Clearances, *Journal of Lubrication Technology* **105**: 120-130.

Khosla, P. K. and Rubin, S. G. (1974). A Diagonally Dominant Second-Order Accurate Implicit Scheme, *Computers and Fluids* **2**: 207-209.

Lipschitz, A., Basu, P. and Johnson, R. P. (1991). A Bi-Directional Gas Thrust Bearing, *Tribology Transactions* **34**(1): 9-16.

Mitsuya, Y. (1993). Modified Reynolds Equation for Ultra-Thin Film Gas Lubrication Using



- 1.5-Order Slip-Flow Model and Considering Surface Accommodation Coefficient, *Journal of Tribology* **115**: 289–294.
- Nguyen, S. H. (1991). p-Version Finite Element Analysis of Gas Bearings of Finite Width, *Journal of Tribology* **113**: 417–420.
- Pinkus, O. and Lund, J. W. (1981). Centrifugal Effects in Thrust Bearings and Seals Under Laminar Conditions, *Journal of Lubrication Technology* **103**: 126–136.
- Ruiz, O. J. and Bogy, D. B. (1990). A Numerical Simulation of the Head-Disk Assembly in Magnetic Hard Disk Files: part 1 - Component Models, *Journal of Tribology* **112**: 593–602.
- Taylor, C. M. and Dowson, D. (1974). Turbulent Lubrication Theory - Application to Design, *Journal of Lubrication Technology* pp. 36–47.
- Venner, C. H. (1991). *Multilevel Solution of the EHL Line and Point Contact Problems*, PhD thesis, University of Twente, The Netherlands.
- Zeeuw, P. M. D. (1990). Matrix-dependent prolongations and restrictions in a blackbox multigrid solver, *Journal of Computational and Applied Mathematics* **33**: 1–27.